First-order aerodynamic and aeroelastic behavior of a single-blade installation setup

M Gaunaa, L Bergami, S Guntur and F Zahle
DTU Wind Energy, Technical University of Denmark
Risø Campus, Roskilde - Denmark

E-mail: macg@dtu.dk

Abstract.
Limitations on the wind speed at which blade installation can be performed bears important financial consequences. The installation cost of a wind farm could be significantly reduced by increasing the wind speed at which blade mounting operations can be carried out. This work characterizes the first-order aerodynamic and aeroelastic behavior of a single blade installation system, where the blade is grabbed by a yoke, which is lifted by the crane and stabilized by two taglines. A simple engineering model is formulated to describe the aerodynamic forcing on the blade subject to turbulent wind of arbitrary direction. The model is coupled with a schematic aeroelastic representation of the taglines system, which returns the minimum line tension required to compensate for the aerodynamic forcing. The simplified models are in excellent agreement with the aeroelastic code HAWC2, and provide a solid basis for future design of an upgraded single blade installation system able to operate at higher wind speeds.

1. Introduction

Modern wind turbines are installed in high wind sites to maximize their power output. This site choice, however, complicates the installation process, as the required lifting equipment can only operate up to a wind speed limit, which, for current state-of-the-art equipment is typically around 8-12 m/s. For higher wind speed all the operations are blocked, with significant economic consequences as the expensive installation equipment (vessels, cranes, yokes, crews, etc.) is kept on-hold. The typical cost of waiting for a low wind speed time window is estimated around 15 million euros for a middle-size offshore wind farm. Single blade installations are performed with a yoke that grabs the blade around its center of mass (COM). For direct drive wind turbines where the hub can not rotate during installation, the yoke has to rotate each blade until the angle imposed by the fixed hub is matched. The yoke is hooked in one point and lifted by a crane. Due to the turbulent wind forcing, the yoke displaces and rotates, thus two taglines connecting the yoke or the blade to the crane are typically used to stabilize the root of the blade until its bolted onto the turbine hub. Current state-of-the-art lifting equipment has no active compensation for the wind forces, thus installation is only possible for wind speeds lower than the specified limits.

This work presents a model of the first-order aerodynamic and aeroelastic behavior of the single blade installation system; the model will provide the basis for future studies on strategies to allow single blade installation in higher winds (e.g. passive design changes, active control,

etc.). In this work, the installation system consists of a yoke that grabs on the blade, and is connected to a (rigid) crane by a lifting cable and two taglines, figure 1.

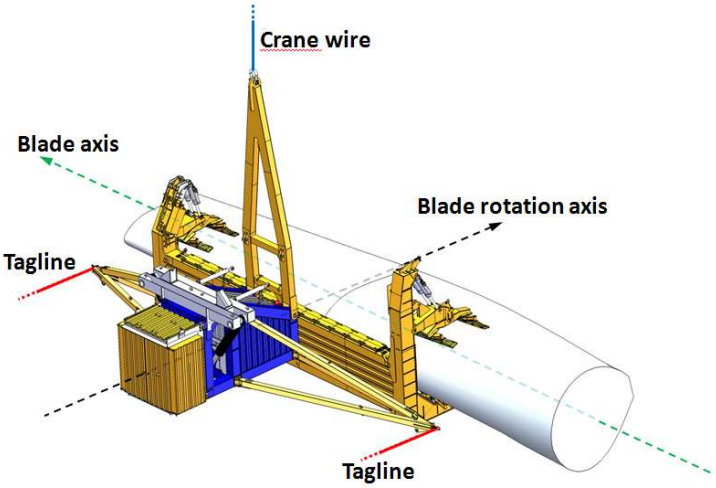

Figure 1. The wind turbine blade held by a blade yoke suspended in a wire (blue) from the crane, and stabilized by two taglines (red) from the yoke to the crane

The paper first proposes a simple engineering model to describe the quasi-steady aerodynamic forces and moments on a wind turbine blade, for turbulent wind with an arbitrary direction in space. An aeroelastic model is then developed to determine the minimum tagline tensions required to stabilize the blade yoke for given blade inclination, wind velocity and direction. Finally, the key behavior of the system is outlined. The blade in the case study presented in this work is taken from the openly available specifications of the DTU 10-MW Reference Wind Turbine (RWT)[1]. The blade is 86.37 m long, weights nearly 42 tonnes, and has a maximum chord of 6.2 m.

2. Models

A novel engineering model to predict the aerodynamic forces and moments on the blade is first presented. Thereafter, the model is coupled to a simple aeroelastic representation of the blade installation system, which returns an estimate of the minimum tagline tension required to compensate for the aerodynamic forcing. The simple models are supported and compared against simulations performed with DTU's aeroelastic code HAWC2 [2]; whereas the CFD method EllipSys3D [3–5] provides the 3D steady aerodynamic characterization of the non-rotating blade. As the investigation concerns a characterization of the first-order behavior, the aerodynamic interference due to the yoke on the blade aerodynamics is here neglected.

2.1. Engineering model for aerodynamic forces on a wind turbine blade under single blade installation

The orientation of the wind turbine blade in space, and thus the direction of the uniform mean wind with respect to the blade, is fully defined by three angles: ν, θ, and η, figure 2. The blade roll angle ν is zero when the blade lies horizontally in the plane defined by the reference axes x (in the spanwise direction), and y (positive toward the trailing edge). The rotation of the wind vector V_∞ in the xy plane is defined by the yaw angle θ; whereas the pitch angle η specifies the rotation of the blade around its spanwise axis. Aerodynamic forces and moments in the following analysis are all defined with respect to the 'global' reference axes xyz, which do not

rotate with the blade. Furthermore, the engineering models assume a completely straight blade.

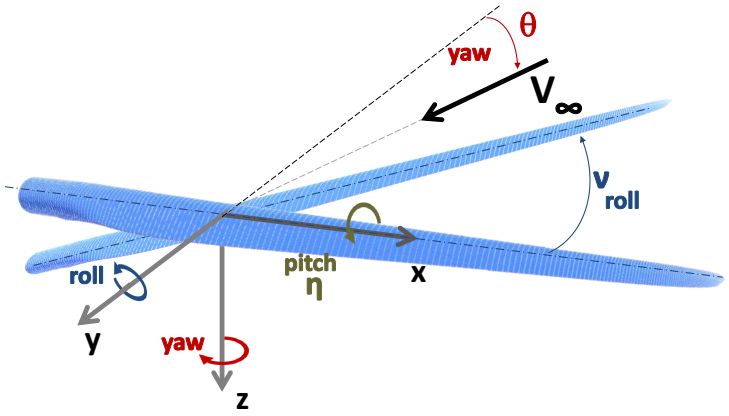

Figure 2. Reference coordinate system and definition of yaw roll and pitch angles. The x, y, z coordinate system is fixed in the global frame of reference and does not move with the blade.

2.1.1. Mean forces and moments The cross-flow principle [6, 7] states that the aerodynamic forces on a 2D structure act as if the spanwise flow velocity component was absent. The principle applies to the aerodynamic forces on a wind turbine blade, where a local 2D approximation of the blade shape is acceptable. Combining the cross-flow principle with the setup geometry (η is the blade pitch, $\xi(r)$ is the blade local twist), the local angle of attack is:

$$\alpha_{loc}(r) = \eta + \xi(r) + \Delta\alpha, \quad \text{and} \quad \Delta\alpha = \arctan 2(\sin\theta \sin\nu, \cos\theta). \tag{1}$$

Note that the variation of angles of attack along the blade stems only from the blade twist, so it is independent of the orientation of the blade with respect to the wind. This mean that the mean integral lift and drag forces[1] turns out to be (in the global coordinate system):

$$\vec{F} = \sqrt{1 - sin^2\theta \cos^2\nu} \begin{bmatrix} -\sin^2\nu \sin\theta & \sin\nu\cos\theta \\ \cos\theta & \sin\nu\sin\theta \\ -\sin\nu\cos\nu\sin\theta & \cos\nu\cos\theta \end{bmatrix} \begin{bmatrix} F_{y\perp} \\ F_{z\perp} \end{bmatrix} \tag{2}$$

Here $F_{y\perp}$ and $F_{z\perp}$ are the integral forces at the perpendicular flow reference condition $\theta = \nu = 0$ at the pitch angle $\eta + \Delta\alpha$

$$F_{y\perp} = +0.5\rho V_\infty^2 A C_D(\eta + \Delta\alpha) \tag{3}$$
$$F_{z\perp} = -0.5\rho V_\infty^2 A C_L(\eta + \Delta\alpha) \tag{4}$$

Note that in case of a 'clean' yawed flow ($-\pi/2 < \theta < \pi/2$) where $\nu = 0$ and therefore also $\Delta\alpha = 0$, the forces scale with $\cos^2\theta$ as they should according to the crossflow principle.

The aerodynamic moment with respect to the y and z axes results from the integration of the local crossflow lift and drag forces along the blade; whereas, for a straight blade, the pitching moment M_x is given by the integration of local 2D moment coefficients. Since both the blade

[1] all in the 'crossflow sense', meaning that they have the direction (and magnitude) they would have had if the spanwise component of the wind was absent

and the crossflow lift and drag directions are known, the moment with respect to the reference position on the blade can be shown to be

$$\vec{M} = \sqrt{1 - sin^2\theta\cos^2\nu} \begin{bmatrix} \cos\nu & -\sin^2\nu\sin\theta & \sin\nu\cos\theta \\ 0 & \cos\theta & \sin\nu\sin\theta \\ -\sin\nu & -\sin\nu\cos\nu\sin\theta & \cos\nu\cos\theta \end{bmatrix} \begin{bmatrix} M_{x\perp}\sqrt{1 - sin^2\theta\cos^2\nu} \\ M_{y\perp} \\ M_{z\perp} \end{bmatrix} \quad (5)$$

In analogy with the force expressions $M_{x\perp}$, $M_{y\perp}$ and $M_{z\perp}$ are the integral moments with respect to the reference position on the blade at the perpendicular flow reference condition $\theta = \nu = 0$ at the pitch angle η

$$M_{x\perp} = 0.5\rho V_\infty^2 A^{3/2} C_{M,x}(\eta + \Delta\alpha) \quad (6)$$

$$M_{y\perp} = 0.5\rho V_\infty^2 A^{3/2} C_{M,y}(\eta + \Delta\alpha) \quad (7)$$

$$M_{z\perp} = 0.5\rho V_\infty^2 A^{3/2} C_{M,z}(\eta + \Delta\alpha) \quad (8)$$

Also in this case the nondimensional coefficients needed for determination of the forces in the general case can therefore be determined once and for all for the wing as function of the pitch angle at the reference perpendicular condition $\nu = \theta = 0$. Note that in most cases $M_{x\perp}$ is negligible compared to $M_{y\perp}$ and $M_{z\perp}$, as the two latter come from forces with a larger (spanwise) distance to the reference position compared to $M_{x\perp}$, for which the distance to the reference position is in the order of the chordlength. As with the forces, in case of a 'clean' yawed flow ($-\pi/2 < \theta < \pi/2$, $\nu = \Delta\alpha = 0$), the moments also scale with $\cos^2\theta$ in agreement with the cross-flow principle.

As mentioned earlier the blade is assumed to be completely straight in this model. It would be possible to include the effect of non-straight blades (for instance prebend etc.), but it is believed that the added accuracy would not justify the penalty in terms of added model complexity of this first-order model.

2.1.2. Standard deviation of forces and moments For single blade installation the time-varying part of the aerodynamic loading is at least as important as the mean part of the loading. The time varying part stems from the motion of the blade and from the turbulent inflow. Since the mass of the system is very large and the eigenfrequency of the first modes in the setup are rather low, it is assumed that the main part of the variation of the aerodynamic forces stems from the turbulent inflow[2]. Under the assumption that the intensity, structure and length scales of the turbulence in the flow are identical in all directions, by combining the cross-flow principle with a linearization of the local quasi-steady forces around their mean flow values, the variation in magnitude of the 'cross-flow' 2D lift and drag forces reads:

$$\begin{bmatrix} F_d - |F_d| \\ F_l - |F_l| \end{bmatrix} = 0.5\rho V_\infty^2 c(r) TI \sqrt{1 - \sin^2\theta\cos^2\nu} \begin{bmatrix} 2C_d(r) & C_d'(r) - C_l(r) \\ 2C_l(r) & C_l'(r) + C_d(r) \end{bmatrix} \begin{bmatrix} f_c(r,t,\nu,\theta) \\ f_n(r,t,\nu,\theta) \end{bmatrix} \quad (9)$$

Here TI is the turbulence intensity, C_d and C_l the 2D lift and drag coefficients, $C_{\cdot}' = \partial C_{\cdot}/\partial\alpha$ and f_c and f_n are non-dimensional quantities that determine the velocity fluctuations in time and space in the chordwise and normal directions; for instance, in the chordwise direction: $u_c(r,t,\nu,\theta) = TI\ V_\infty f_c(r,t,\nu,\theta)$. Since the characteristics of the turbulent structures in the flow are assumed to be identical in all directions, and the correlations of the velocity fluctuations in the chordwise and normal directions are assumed to be independent of blade orientation (ν and η) and wind direction (θ), the standard deviation of the integral forces in the 'crossflow lift'($\vec{e}_L$),

[2] The unsteady loading corresponding to vortex shedding is neglected in this work.

'crossflow drag'($\vec{e}_D$) and span ($\vec{e}_S$) directions

$$\vec{e}_L = \frac{\begin{bmatrix} -\sin\nu\cos\theta \\ -\sin\nu\sin\theta \\ -\cos\nu\cos\theta \end{bmatrix}}{\sqrt{1-sin^2\theta\cos^2\nu}} \qquad \vec{e}_D = \frac{\begin{bmatrix} -\sin^2\nu\sin\theta \\ \cos\theta \\ -\sin\nu\cos\nu\sin\theta \end{bmatrix}}{\sqrt{1-sin^2\theta\cos^2\nu}} \qquad \vec{e}_S = \begin{bmatrix} \cos\nu \\ 0 \\ -\sin\nu \end{bmatrix} \tag{10}$$

turns out to be

$$\begin{bmatrix} \mathrm{std}(F_L) \\ \mathrm{std}(F_D) \\ \mathrm{std}(F_S) \end{bmatrix} = \rho V_\infty^2 TI\, A\sqrt{1-sin^2\theta\cos^2\nu} \begin{bmatrix} K_{Fz\perp} \\ K_{Fy\perp} \\ 0 \end{bmatrix} \tag{11}$$

Under the stated assumptions of linearity and isotropic turbulence, for a given blade, the non-dimensional coefficients $K_{Fy\perp}$ and $K_{Fz\perp}$ are only functions of the blade equivalent 2D pitch: $\eta + \Delta\alpha$. At reference conditions with $\nu = \theta = 0$, they are determined as:

$$K_{Fy\perp} = \frac{\mathrm{std}\left(F_{y\perp}(\eta+\Delta\alpha)\right)}{\rho V_\infty^2 TI\, A}\Big|_{ref}, \quad \text{and} \quad K_{Fz\perp} = \frac{\mathrm{std}\left(F_{z\perp}(\eta+\Delta\alpha)\right)}{\rho V_\infty^2 TI\, A}\Big|_{ref} \tag{12}$$

Since the moment around the blade reference point also results from integration of the local lift and drag forces, eq. (9), the standard deviation of the aerodynamic moments along the directions given in Equation 10 is similarly formulated as:

$$\begin{bmatrix} \mathrm{std}(M_L) \\ \mathrm{std}(M_D) \\ \mathrm{std}(M_S) \end{bmatrix} = \rho V_\infty^2 TI\, A^{3/2}\sqrt{1-sin^2\theta\cos^2\nu} \begin{bmatrix} K_{Mz\perp} \\ K_{My\perp} \\ K_{Mx\perp} \end{bmatrix} \tag{13}$$

Where, in analogy with the force case, the non-dimensional coefficients $K_{Mx\perp}$, $K_{My\perp}$ and $K_{Mz\perp}$ are given from a reference condition $\nu = \theta = 0$ case as

$$K_{Mx\perp} = \frac{\mathrm{std}\left(M_{x\perp}(\eta+\Delta\alpha)\right)}{\rho V_\infty^2 TI\, A^{3/2}}\Big|_{ref} \tag{14}$$

$$K_{My\perp} = \frac{\mathrm{std}\left(M_{y\perp}(\eta+\Delta\alpha)\right)}{\rho V_\infty^2 TI\, A^{3/2}}\Big|_{ref} \tag{15}$$

$$K_{Mz\perp} = \frac{\mathrm{std}\left(M_{z\perp}(\eta+\Delta\alpha)\right)}{\rho V_\infty^2 TI\, A^{3/2}}\Big|_{ref} \tag{16}$$

Note that, as for the mean loads, in most cases $K_{Mx\perp}$ is negligible compared to $K_{My\perp}$ and $K_{Mz\perp}$. As for the mean values, the standard deviation of integral forces and moments scales linearly with density, and quadratically with wind speed. Furthermore, the standard deviation of the forces and moments scale linearly with the turbulence intensitiy, and for a 'clean ' yaw case $\nu = 0$, the standard deviation scales with $|\cos\theta|$: the standard deviation of the forces thus decreases at a slower rate with yaw angle than the mean forces do. It is possible to express the standard deviation of the forces and moments in the global directions (x, y,z) by use of correlation functions determined for the reference condition, but this development is left as a future work.

In the derivation of the model, linearization is used. For this to be a good approximation, the magnitude of the disturbances relative to the mean value should be small. Since the magnitude of the effective velocity in the direction perpendicular to the span direction is $V_{\infty,\perp} = V_\infty\sqrt{1-\sin^2\theta\cos^2\nu}$ and the turbulent fluctuations remains constant, the effective turbulence intensity seen by the cross-sections is $TI_{eff} = TI/\sqrt{1-\sin^2\theta\cos^2\nu}$. The linearization is a

good approximation as long as TI_{eff} is below unity. The model does not say anything about the frequency content, but the assumption of the given turbulence structures indicate that the frequency corresponding to a specific size of the turbulent structures in the flow scales linearly with the convection velocity. For instance, if measurements or simulations show a peak in the aerodynamic loads at 1.2 Hz at $V_\infty = 5$ m/s, this peak would move to 2.4 Hz at $V_\infty = 10$ m/s.

2.2. A Generalized Aereolastic Engineering Model

The generalized aeroelastic model of the single blade installation system consists of the stiff blade, the yoke, the lifting cable to the crane top, and the taglines. For a specified wind direction, blade orientation and tag-lines angle, the model allows to determine whether the system has a steady equilibrium, and what the minimum required tension in the tag-lines would be to maintain the steady equilibrium. The parameters considered in the model are: the wind direction ($-90^\circ < \theta < 90^\circ$), the blade pitch ($\eta$) and roll angle ($-90^\circ < \nu < 90^\circ$), and the angle the taglines form with the ground (ψ), which is currently fixed to $\psi = 0$, corresponding to tag-lines in the horizontal plane.

For the system to be in equilibrium, the sum of all forces on the blade in each of the three directions (x, y and z) and the sum of all moments about the clamping point must all be zero. With the these six equations and the additional constraint of positive tagline tension $\{T_0, T_1, T_2\} \geq 0$, the model returns the minimum values of the tensions T_1, T_2 required for a static equilibrium, and the angles the cables would make with the z and y axes.

2.3. HAWC2

HAWC2[2] is a time marching aeroservoelastic simulation code developed at DTU Wind Energy. The code is based on a multi-body formulation, and the structure of the blade is modeled as a sequence of Timoshenko beam elements with the properties specified by Bak et al.[1]. The code is usually used for wind turbine aeroelastic load simulations, but it is very generally formulated. Therefore it is possible to simulate also for instance the single blade installation setup. In this case the aerodynamics are looked up independently at each blade section[3], using the steady aerodynamic input from EllipSys, and a Beddoes-Leishmann dynamic stall model [8]. Two model configurations are considered here: *Flex.Ds.* accounts for the blade flexibility and unsteady aerodynamics, and a simpler configuration *Stiff.Qs*, where the blade is approximated to a rigid structure and the aerodynamic model is simplified to a steady look-up. Simulations are performed in uniform flow, and for turbulent wind fields generated using Mann's [9] model. The default configuration considers a mean wind speed of 10 m/s, and a turbulence intensity of 0.12, representative of an offshore site.

2.4. EllipSys

3D CFD simulations were carried out to derive 2D airfoil data for a single blade at standstill. 2D airfoil data are needed as input to HAWC2 to be able to simulate the response to turbulent inflow. The unsteady simulations were done using the incompressible Navier-Stokes flow solver EllipSys3D [3–5] on a spherical mesh with 7.8 mill. cells. The total simulation time was 100 sec with an averaging time of 40 sec. The turbulence was modeled using Detached Eddy Simulation to resolve the unsteady vortex shedding on the blade at standstill.

3. Results

In this section, the methods described in the previous section will be validated and used to illuminate key factors in the single blade installation setup.

[3] disabling the BEM based rotor aerodynamics used in standard HAWC rotor computations

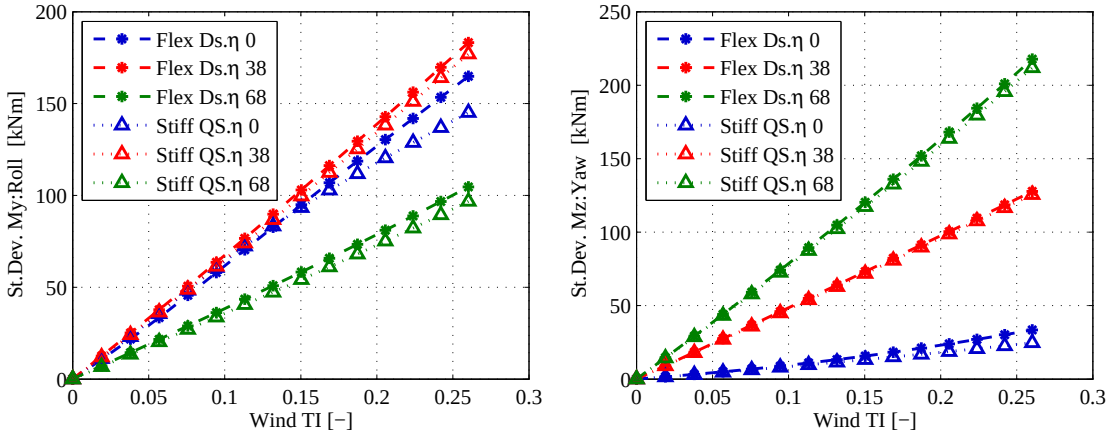

Figure 3. HAWC2 aeroelastic simulations at different wind turbulence intensities for $\theta = \nu = 0$. Left: Roll moments, My. Right: Yaw moments, Mz.

3.1. Validation of aerodynamic engineering model

The aerodynamic engineering model was validated with results from the aeroelastic code HAWC2. It was verified that:

- Mean aerodynamic forces and moments scale with ρV_∞^2.
- Mean aerodynamic forces and moments scale with the square cosine of the wind yaw angle, see section 3.3.
- Standard deviation of forces and moments scale with ρV_∞^2.
- Standard deviation of forces and moments scale linearly with turbulence intensity, see section 3.2.
- Standard deviation of forces and moments scale with the absolute value of the cosine to the wind yaw angle, see section 3.3

3.2. Load variation and Turbulence Intensity

As a first-order approximation, the aerodynamic engineering model indicates that the standard deviation of the aerodynamic loads scales linearly with the turbulence intensity of the wind field, eqs. (11) and (13). The hypothesis is verified against HAWC2 simulations in a 3D turbulent wind field [9] of varying turbulence intensity, figure 3. The results confirm a linear dependency of the standard deviation of the aerodynamic loads with the turbulence intensity; the linear slope is generally steeper for blade pitch angles that returns higher mean aerodynamic loads, but higher standard deviations in the loads may occur in some cases also for cases with lower mean values. This is caused by changes in angle of attack along the blades, which in the cases with high force coefficient slopes result in higher unsteady loading. The linear trend in the load variation magnitudes with respect to turbulence intensity is outlined both in the case of a flexible blade model with unsteady aerodynamics (*Flex.Ds.*), and in the simplified stiff blade model with Quasi-Steady aerodynamics (*Stiff.Qs.*). This indicates that the assumption of a stiff blade and quasisteady aerodynamics is adequate in this case where the blade is rigidly clamped in its COM.

3.3. Yawed inflow

As the wind direction is varied in the horizontal plane (i.e. the yaw angle, θ, is changed in figure 2, $\nu = 0$), the engineering model predicts that the mean load level scales with the square

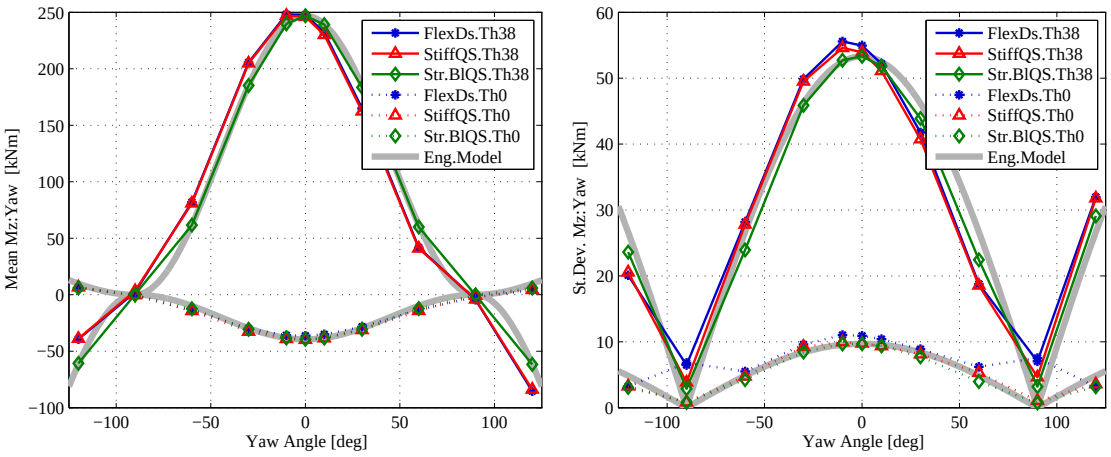

Figure 4. Aerodynamic loads for varying inflow yaw angles, θ, comparison of HAWC2 and engineering model. Left: Mean yaw moment. Right: Standard deviation of yaw moment. Mean wind speed 10 m/s, $TI = 0.12.$, horizontal blade $\nu = 0$.

cosine of the yaw angle, eq.(2) and (5), whereas the standard deviation of the aerodynamic loads varies linearly with the yaw cosine, (11) and (13). The largest loads, and the highest load variations are hence reported for wind directions perpendicular to the blade ($\theta = 0$). The analytical trend is confirmed by HAWC2 simulations, figure 4. Minor discrepancies are mainly caused by the prebend of the blade and disappear once the blade is assumed to be straight and rigid (*Str.Bl.QS.* model configuration).

3.4. Steady and unsteady aerodynamic forces during single blade installation
HAWC2 simulations are performed for the blade clamped at different pitch angles, and wind direction perpendicular to the blade span ($\theta = 0$). The aerodynamic loads, generated either by distributed lift (rolling moment My) or drag forces (yawing moment Mz), vary significantly with the blade pitch angle, figure 5. Furthermore, when the wind speed variation caused by atmospheric turbulence is taken into account, the reported maximum aerodynamic loads are significantly larger than what would result by considering only a constant wind flow equal to the 10 minutes average one, marks in figure 5.

3.5. On the importance of unsteady aerodynamic effects and blade flexibility.
Previous figures have shown that the simpler HAWC2 *Stiff.Qs.* model predicts aerodynamic loads similar to the more accurate *Flex.Ds.*. The two model configurations are now compared for the blade response to structural forcing; the forcing is generated by prescribing harmonic rolling oscillations of the blade around its COM, and the response is measured in terms of reaction moment M_y. The My responses for the elastic model configurations show a peak at frequencies close to 0.73 Hz, the first flapwise frequency of the blade clamped at its COM. The peak is damped by the aerodynamic forces, and is not captured by the stiff model configurations, which hence returns response predictions similar to the flexible model ones only for frequencies up to 0.4 Hz (nearly 55% of the natural frequency). The simpler model configuration *Stiff.Qs.* would hence return a valid approximation of the structural response only if the rigid motions that the blade will undergo during mounting (e.g. from dangling of the yoke) have prevailing frequencies which are lower than 0.4 Hz.

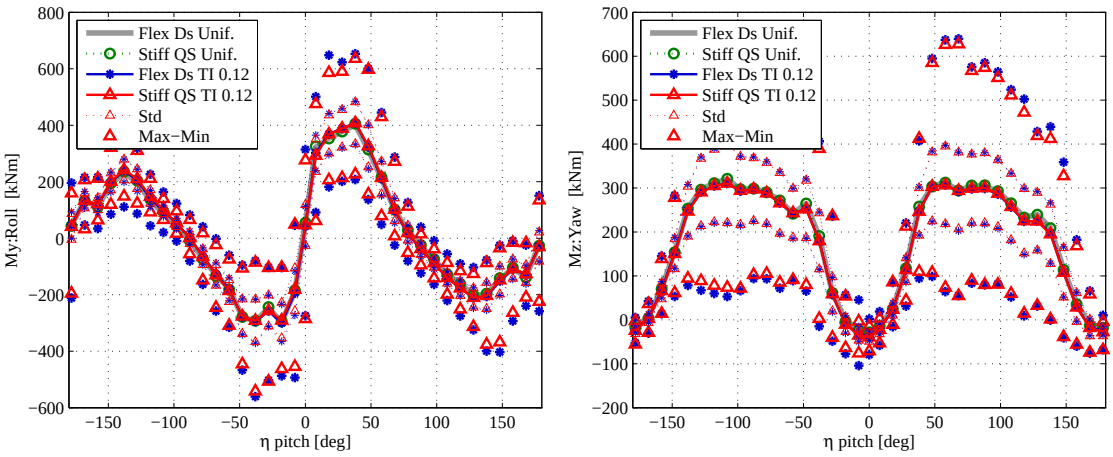

Figure 5. HAWC2 aeroelastic simulation of the aerodynamic roll and yaw moments with respect to the blade COM for different blade pitch angles.

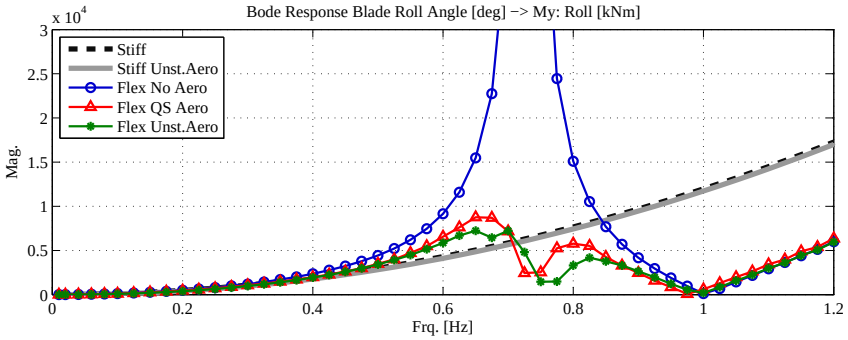

Figure 6. Aeroelastic response of the clamped blade to harmonic rolling oscillations; magnitude of the rolling moment reaction at the clamping point.

3.6. Generalized aeroelastic engineering model: minimum tagline tensions

The results in this subsection are based on a total mass of $M = 100000$ kg, tagline arm length $l_t = 10$ m and distance from COM to crane cable attachment $l_c = 10$ m. From the results of the generalized aeroelastic engineering model of the single blade installation system it is observed that:

- The tag-line tensions scale as V_∞^2. This is a direct result of the aerodynamic forces being proportional to V_∞^2, and is expected to hold also in turbulent conditions: the maximum tagline tension thus scales with the square of the maximum expected wind speed.
- For the system to be in equilibrium, the minimum tension in one of the tag-line tensions is always zero. Hence, the contour plots in figure 7 simply indicate the tension of *one* of the tag-lines. Therefore the contours also indicate the moment transferred to the structure that holds the other end of the taglines.
- In order to withstand additional aerodynamic forces due to turbulence the tensions in the tag-lines must be greater than the minimum values computed herein.
- Figure 7 shows an example of the $\min(T_1 + T_2)$ contours at blade pitch $\eta = 0°$ (left) and $\eta = 45°$ (right). The θ and ν combination at which the lowest tagline tension is reported (dark blue) changes significantly depending upon the pitch angle η. Given θ and ν there

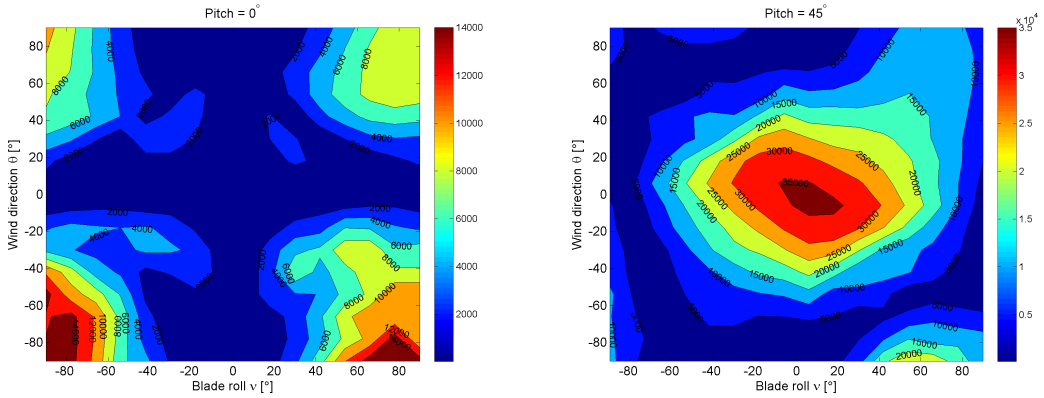

Figure 7. Contour lines of $\min(T_1 + T_2)$ (in [N]) for blade pitch $\eta = 0^o$ (left) and $\eta = 45^o$ (right), at $V_\infty = 10$ m/s .

is hence a pitch angle η that minimizes the required tagline tension: e.g. $\eta = 0$ would be preferable for blade mounting conditions with $\theta = 0°$ and $\nu = 0°$.

- The figures also show that the tension in the tag-lines varies greatly - from a few hundred Newtons to several thousand Newtons, over the considered range of θ and ν angles. According to the restrictions that a real mechanism has on the maximum possible tag-line tension the crane can handle, the model might also indicate which conditions might be unbearable for the single blade installation system.

4. Conclusion

The 10 minute average wind speed at the site is not a conclusive parameter to determine whether a blade mounting operation can be carried out. In fact, the wind direction with respect to the blade, the blade orientation, and the turbulence intensity largely affect the aerodynamic loads. The proposed engineering model returns an analytical relation that allows to scale the aerodynamic loads as function of key site parameters: wind speed and density, turbulence intensity, wind and blade orientation. The mean aerodynamic load generally scales with $\rho V_\infty^2 \cos^2\theta$, whereas its standard deviation with $\rho V_\infty^2 \mathrm{TI} |\cos\theta|$. The aerodynamic load predictions from the engineering model have proved in excellent agreement with HAWC2 results, and combined with a simplified model of the yoke tagline system allow to quickly obtain a prediction of the forces the tag line systems will have to counteract. The prediction model can be used either to determine whether the mounting operation can be carried out in some specific site conditions, or to determine which blade orientation would be preferable for a specific wind direction. In general, the highest aerodynamic loads, and hence tagline tensions, are reported for blade pitch angles where the drag prevails ($30° < \pm\eta < 150°$), and for wind directions perpendicular to the blade span axis.

5. Future work

The present work is limited to a first-order steady characterization of the single blade installation system, and the aerodynamic forces it undergoes. Future investigations will verify the validity of the aerodynamic crossflow principle, which also underlies the HAWC2 model, against 3D CFD computations. CFD methods will also be employed to assess the importance of vortex-shedding dynamics, as well as the effects of the aerodynamic forces and flow disturbances generated by the presence of the blade yoke. The model of the single blade installation system will be then expanded to account also for the cable dynamics. Finally, the model will be employed to simulate

the entire installation/lift in time, and devise control strategies and design modifications that would allow an upgraded single blade installation system to operate in higher wind speeds.

Acknowledgements
It is gratefully acknowledged that this work was funded by the Danish Energy Agency within the project "Single Blade Installation in high Wind Speeds".

References

[1] Bak C, Zahle F, Bitsche R, Kim T, Yde A, Henriksen L, Andersen P B, Natarajan A and Hansen M H 2013 *Wind Energy* **To be accepted**
[2] Larsen T J 2009 How 2 HAWC2 the user's manual Tech. Rep. R-1597(EN) Risoe National Laboratory. Technical University of Denmark
[3] Michelsen J A 1992 Basis3D—a platform for development of multiblock PDE solvers Tech. Rep. Tech. Rep. AFM 92-05 Technical University of Denmark
[4] Michelsen J A 1994 Block structured multigrid solution of 2D and 3D elliptic PDEs Tech. Rep. Tech. Rep. AFM 94-06 Technical University of Denmark
[5] Sørensen N N 1995 General purpose flow solver applied to flow over hills Tech. Rep. Ris-R-827-(EN) Risoe National Laboratory.
[6] Hoerner S 1965 Fluid-dynamic drag Tech. rep. Hoerner Fluid Dynamics; Bricktown New Jersey
[7] Hoerner S and Borst H 1975 Fluid-dynamic lift Tech. rep. Hoerner Fluid Dynamics; Bricktown New Jersey
[8] Hansen M H, Gaunaa M and Madsen H A 2004 A Beddoes-Leishman type dynamic stall model in state-space and indicial formulations Tech. Rep. R-1354(EN) Risoe National Laboratory, Roskilde (DK)
[9] Mann J 1998 *Probabilistic Engineering Mechanics* **13** 269–282 ISSN 0266-8920